JOC The Journal of Organic Chemistry

Article

pubs.acs.org/joc

Twisting-Based Spectroscopic Measure of Solvent Polarity: The P_T Scale

Wei-Jen Lo, Yi-Hui Chen, and Kuangsen Sung*

Department of Chemistry, National Cheng Kung University, No. 1 University Road, Tainan 700, Taiwan

Supporting Information

ABSTRACT: The P_T scale, which is correlated well with the $E_T(30)$, Y, and Z scales, is the first twisting-based spectroscopic measure of solvent polarity. It is based on two combined mechanisms: (1) the solvent-dependent intramolecular charge-transfer absorption that displays a regular hypsochromic band shift in polar solvents and (2) overcoming the intramolecular hydrogen-bond of *o*-**1** by its differentiated solvation in polar solvents, causing a C−C bond to twist that leads to a regular hypsochromic shift of its lowest energy electronic absorption band.

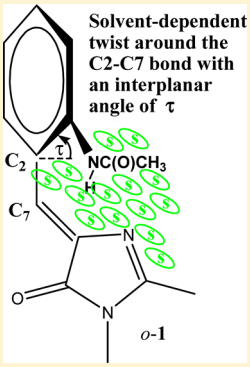

INTRODUCTION

Solvents can significantly influence reaction rates, the position of chemical equilibria, and absorption and emission spectra involving electronic, vibrational, and rotational transitions. These solvent effects have been usually understood in terms of solvent polarity. Solvent polarity can be defined as the overall solvation capability (solvation power).[1] The solvation power involves nonspecific dipole/dipole and dipole/induced dipole solute/solvent interactions, as well as specific hydrogen-bond and electron-pair-acceptor (EPA)/electron-pair-donor (EPD) solute/solvent interactions at a molecular microscopic level. Therefore, macroscopic physical solvent parameters such as relative permittivity (ε_r) and refractive index (n) and molecular microscopic physical solvent parameters such as permanent dipole moment (μ) fail to accurately describe the polarity of the solute-surrounding local solvation shell.[1] Thus, some empirical parameters of solvent polarity have been developed as follows.

The desmotropic constants (L),[2] based on a solvent-dependent chemical equilibrium derived from the tautomerization of ethyl acetoacetate as a reference, empirically measure the solvents' enolization capability. The Y scale,[3] based on solvent-dependent reaction rates with the solvolysis of 2-chloro-2-methylpropane as a standard reaction, empirically measures the solvent ionizing power in terms of the solvent influence on build-up of positive charge of a solute during solvolysis. However, the Y scale can be measured only for a limited number of solvents. The Z scale,[4] which was based on electronic absorption of 1-ethyl-4-(methoxycarbonyl)-pyridinium iodide in various solvents, empirically measures the ionizing power of solvents in terms of the influence of the solvent on an intermolecular charge-transfer absorption. However, because of the low solubility of the salt, the Z values for nonpolar solvents are difficult to get. The $E_T(30)$ scale,[1] which was based on absorption of 2,6-diphenyl-4-(2,4,6-triphenylpyridinium-1-yl)phenolate in various solvents, empirically measures the ionizing power of solvents in terms of solvent influence on an intramolecular charge-transfer absorption. The $E_T(30)$ scale is available for a wide range of solvents and it is one of the most useful and widely accepted empirical parameters of solvent polarity. The χ_R scale,[5a] χ_B scale,[5a] π^* scale,[5b] π^*_{azo} scale,[5c] and E^*_{LMCT} scale[5d] are useful empirical parameters of solvent polarity that are based on intramolecular charge-transfer absorption.

Fluorescent dyes with conjugated donor−acceptor systems are another kind of molecules that may sense solvent polarity through solvent-dependent fluorescence emissions in a variety of solvents.[6] This type of molecule undergoes a photoinduced intramolecular charge transfer (PCT), so that their charge-transfer excited states are usually much more polar than the corresponding ground states. According to the Franck−Condon principle, light absorption occurs with a vertical transition of an electron within femtoseconds, followed by solvent reorganization in the range of picoseconds before fluorescent light emits in nanoseconds.[7] Before fluorescent light emits, the charge-transfer excited-states have sufficient time to interact with the surrounding solvent molecules to reach the solvent-stabilized excited-states. Hence, fluorescent emission of this type of molecules provides one of the best ways to sense solvent polarity. The most popular application for this type of fluorescent dyes is the visualization of cell and protein structures.[8]

In this paper, we designed as a prototype molecule the merocyanine dye *o*-**1** of twisting-based spectroscopic indicator

Received: March 20, 2013
Published: April 23, 2013

dx.doi.org/10.1021/jo400586w | J. Org. Chem. 2013, 78, 5925−5931

for solvent polarity (Figure 1). This merocyanine dye *o*-**1** is composed of two rings, an *o*-acetaminophenyl electron-donor

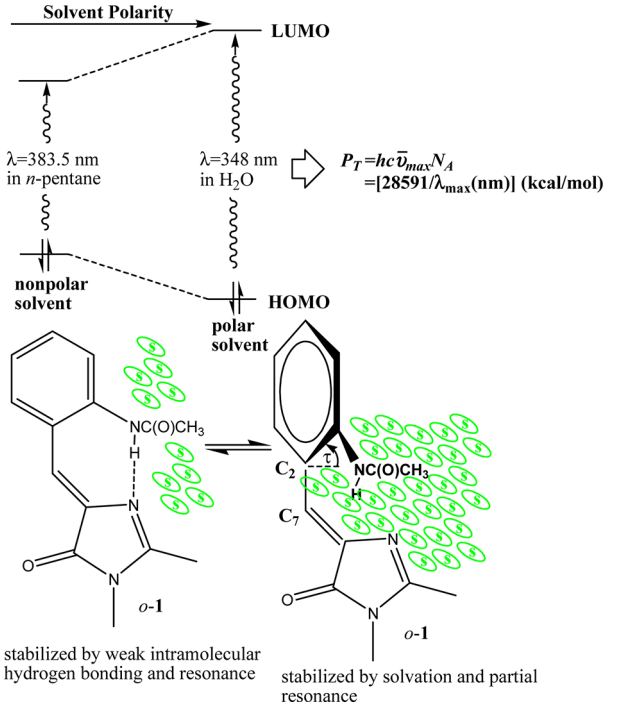

Figure 1. Brief description of the solvent influence on the electronic absorption of planar *o*-**1** and its twisted conformation and definition of the molar transition energy, P_T (twisting-based polarity).

and an imidazolone electron-acceptor moiety, with an additional intramolecular hydrogen bond as a special feature. These two rings are connected together in two ways by conjugated bonding and intramolecular hydrogen bonding. In solvents with various polarities, the solvation of this indicator influences its intramolecular hydrogen bonding for better stabilization. If the solvation overcomes the intramolecular hydrogen bonding, the two rings of the indicator get twisted around the C_2-C_7 bond with an interplanar angle of τ, leading to a decrease of resonance within the conjugated π-system. Hence, we expect that the lowest energy electronic absorption band of this indicator dye is blue-shifted in polar solvents. In this paper, we show that the blue-shift degree of this indicator in polar solvents is proportional to their corresponding solvent polarity. We do not expect that this empirical parameter of solvent polarity would be better than the $E_T(30)$ scale, but we hope it can trigger the generation of even better twisting-based spectroscopic indicators for solvent polarity in the future.

COMPUTATIONAL DETAILS

All calculations reported here were performed with the Gaussian 03 program.[9] Geometry optimization of *o*-**1** was carried out at the B3LYP/6-31+G* level without any symmetry restriction. After the geometry optimization was performed, an analytical vibration frequency was calculated at the same level to determine the nature of the located stationary point. Time-dependent density functional theory (TDDFT) was used to calculate the first five vertical electronic transitions of *o*-**1** in the gas phase and the electron-density surfaces of its molecular orbital at the level of B3LYP-TD/cc-PVDZ//B3LYP/6-31+G*.

RESULTS AND DISCUSSION

Preparation of *o*-**1** was done by treating (*Z*)-4-(2-aminobenzylidene)-1,2-dimethyl-(1*H*,4*H*)-imidazol-5-one (*o*-**ABDI**)[10] with 2 equiv of acetic anhydride (Scheme 1).

Scheme 1. Synthesis of *o*-1 from *o*-ABDI

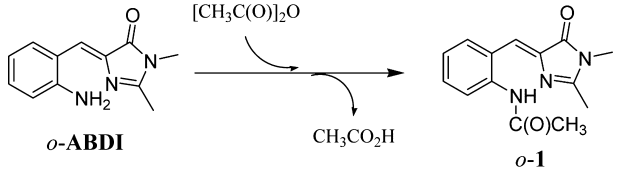

According to the crystal structure of *o*-**1** obtained through X-ray diffraction, the imidazolone and the *o*-acetaminophenyl ring almost stay in a planar conformation with the interplanar angle of ∠N(2)−C(8)−C(2)−C(1) = 0.19° (Figure 2). The distance

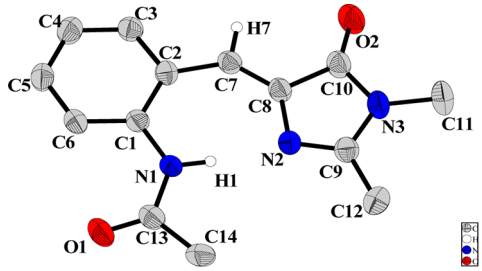

Figure 2. X-ray single-crystal molecular structure of *o*-**1** with thermal ellipsoids at the 50% probability level.

of H(1)···N(2) between the *o*-acetaminophenyl and the imidazolone ring is 185 pm, which corresponds to a hydrogen bonding distance, with ∠N(1)−H(1)−N(2) = 170.7° and N(1)−N(2) = 275 pm. Hence, in the crystal lattice, a seven-membered ring with an intramolecular hydrogen-bond through N(1)−H(1)···N(2) is formed, which is strongly supported by its ^{1}H NMR spectrum in $CDCl_3$, where the signal at δ 12.34 for H(1) on N(1) is significantly downfield-shifted.

The lowest energy electronic absorption band of *o*-**1** measured in acetonitrile is located at λ = 365 nm (ε = 1.29 × 10^4 M^{-1} cm^{-1}), which is hypsochromically shift in polar solvents. We did calculations on the electronic transitions of *o*-**1** at the B3LYP-TD/cc-PVDZ//B3LYP/6-31+G* level to understand whether the lowest energy electronic absorption band involves a charge-transfer transition. The calculated lowest energy singlet electronic transition of *o*-**1** is contributed by 0.59[HOMO → LUMO] − 0.27[HOMO-1 → LUMO] and located at λ = 397 nm with an oscillator strength (*f*) of 0.2658 and a transition electric dipole moment of −1.79 au (−4.55 D) along the *x* axis and −0.51 au (−1.30 D) along the *y* axis, which is in good agreement with the experimental data (λ_{max} = 383.5 nm in *n*-pentane with ε = 1.3 × 10^4 M^{-1} cm^{-1}, which corresponds to an oscillator strength (*f*) of 0.28 according to the equation[7] of $f = 4.3 \times 10^{-9} \int \varepsilon d\nu = 4.3 \times 10^{-9} \varepsilon_{max} \Delta\nu_{1/2}$). The magnitude of this transition electric dipole moment is larger than those of the charge-transfer transitions of nitrobenzene and peridinin (3.2 D for nitrobenzene[11a] and 3.4 D for peridinin[11b]). Hence, we suggest that the lowest energy electronic absorption of *o*-**1** involves a charge-transfer transition. The negative sign of this transition electric dipole moment of *o*-**1** indicates that a substantial electron transfer

dx.doi.org/10.1021/jo400586w | *J. Org. Chem.* 2013, 78, 5925−5931

from the imidazolone moiety to the *o*-acetaminophenyl moiety occurs during excitation (Figure 3). This causes the dipole

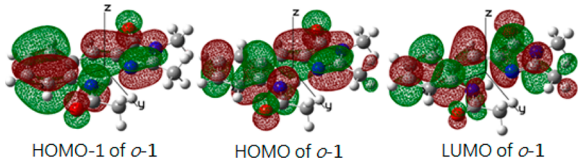

Figure 3. Electron-density surfaces of HOMO-1, HOMO, and LUMO of *o*-**1**.

moment of the first singlet Franck−Condon excited state to be smaller than that of the ground state.[12] This might be one of reasons that make the lowest energy absorption band of *o*-**1** display a regular hypsochromic band shift in polar solvents. However, the lowest energy electronic absorption of *o*-**ABDI**, whose structure is very close to that of *o*-**1**, does not display a regular hypsochromic band shift in polar solvents, even though it also involves a charge-transfer transition that has a substantial electron transfer from the imidazolone moiety to the aniline moiety during excitation.[10] In addition, the lowest energy electronic absorption band of *p*-**1** is not shifted with increasing solvent polarity.[13] This implies that an additional mechanism may be applied to the regular hypsochromic shift of the lowest energy electronic absorption band of *o*-**1** in polar solvents.

We propose that the additional mechanism for the regular hypsochromic shift of the lowest energy electronic absorption band of *o*-**1** in polar solvents is based on the first-order perturbation theory that describes the influence of bond twisting on the HOMO and LUMO energies of a conjugated π-system.[14] If the HOMO is antibonding and the LUMO is bonding in the twisted bond, the bond twisting stabilizes the HOMO but destabilizes the LUMO. On the other hand, if the HOMO is bonding and the LUMO is antibonding in the twisted bond, the bond twisting destabilizes the HOMO but stabilizes the LUMO. According to the DFT calculations of *o*-**1** at the level of B3LYP/cc-pVDZ//B3LYP/6-31+G*, its HOMO and HOMO-1 are antibonding and its LUMO is bonding in the C_2-C_7 bond, so the bond twisting around the C_2-C_7 bond stabilizes its HOMO and HOMO-1 but destabilizes its LUMO, leading to the hypsochromic shift of the intramolecular charge-transfer $\pi-\pi^*$ transition.

What conditions would make *o*-**1** twisted around the C_2-C_7 bond? To answer this question, we need to know what the forces are to drive *o*-**1** to be a flat molecule. Obviously, these forces are intramolecular hydrogen bonding according to N(1)−H(1)···N(2) and through-molecule π-conjugation. Hence, to twist *o*-**1** around the C_2-C_7 bond, the intramolecular hydrogen bond must be weakened and the through-molecule π-conjugation must be reduced, and both of them cost energy. It is known that intramolecular hydrogen bonding within peptides can be overcome by intermolecular hydrogen bonding with water[15] and ionic bonding within ionic salts can be overcome by solvation with water.[16] Hence, we suggest that solvation of *o*-**1** may weaken its intramolecular hydrogen bonding and through-molecule π-conjugation to a certain degree, and that causes *o*-**1** twisted around the C_2-C_7 bond to a certain interplanar angle of τ. According to the first-order perturbation theory, the twist angles (τ) of *o*-**1** in various solvents might be detected by its electronic absorptions in various solvents.

According to the chemical principle of "like dissolves like", *n*-pentane is unlikely to separate the *o*-acetamino moiety of *o*-**1** from its hydrogen-bonded imidazolone moiety by solvation, so the intramolecular hydrogen bond should remain intact in *n*-pentane and its structure in *n*-pentane is supposed to be very similar to its single-crystal molecular structure with a fully extended and conjugated π-system across both *o*-acetaminophenyl and imidazolone moieties, resulting in a red-shift of its lowest energy electronic absorption band to a longer wavelength of λ = 383.5 nm. This lowest energy electronic absorption band of *o*-**1** is regularly blue-shifted as the polarity of the solvent increases (Table 1). It reaches the largest blue-shift in water with the maximum blue-shift of $\Delta\lambda$ = 35.5 nm, as compared to *n*-pentane.

The hypsochromic band shift also happens to the emission maximum of *o*-**1** in polar solvents, but the largest blue-shift is only $\Delta\lambda$ = 11 nm, which is much less than that found for its electronic absorption spectra (Table 1). This is because the excited state from which emission of *o*-**1** occurs is not a Franck−Condon excited state but a solvent-stabilized equilibrium excited state.[7] The Franck−Condon ground state to which emission of *o*-**1** leads is not solvent-stabilized,[7] but it is destabilized as compared to the solvent-stabilized equilibrium ground state, from which the electronic absorption of *o*-**1** occurs. In addition to the smaller blue-shift degree, the fluorescence quantum yield of *o*-**1** is quite low, so the emission maximum of *o*-**1** is not a suitable indicator for solvent polarity.

The lowest energy electronic absorption of *o*-**1** has been measured in 51 common solvents at a concentration of 3.0×10^{-5} M, which include alkanes, alkenes, cycloalkanes, cycloalkenes, haloalkanes, alkylarenes, heteroarenes, aliphatic monoalcohols, an aliphatic polyalcohol, aliphatic and cycloaliphatic ethers, aliphatic ketones, carboxylic acid and anhydride, aliphatic and aromatic esters, amides, aliphatic nitriles, aliphatic and aromatic amines, phosphorus compounds, sulfur compound, water, and heavy water. The 51 solvents are evenly distributed from nonpolar to polar solvents. The solubility of *o*-**1** in all 51 solvents is good and sufficient for the electronic absorption measurement. The molar absorption coefficients of *o*-**1** in these 51 solvents are all very similar, and their values are around $\varepsilon = 1.3 \times 10^4$ $M^{-1}cm^{-1}$. The lowest energy electronic absorption maximum of *o*-**1** can be converted into the corresponding molar transition energy, P_T (twisting-based polarity), with the equation of $P_T = hc\bar{\upsilon}_{max}N_A = [28591/\lambda \text{ max(nm)}]$ (kcal/mol) with c = light speed and N_A = Avogadro's number. As the solvent polarity increases from *n*-pentane to water, the P_T values regularly increase from 74.55 to 82.16. (ΔP_T = 7.61 kcal/mol).

Both the P_T and the $E_T(30)$[1c] scale register nonspecific dipole/dipole and dipole/induced dipole solute/solvent interactions very well. For example, replacement of an alkyl group by the corresponding alkenyl group usually increases its polarity, such as, for example, cyclohexane (P_T = 74.65, $E_T(30)$ = 30.9) versus cyclohexene (P_T = 76.04, $E_T(30)$ = 32.2); 1-propanol (P_T = 79.22, $E_T(30)$ = 50.7) versus allyl alcohol (P_T = 80.31, $E_T(30)$ = 51.9). It is likely that the polarizability of the electron cloud of a π bond is higher than that of a σ bond. Replacement of a bromo atom by a chloro atom usually increases the polarity, such as dibromomethane (P_T = 76.04, $E_T(30)$ = 39.04) versus dichloromethane (P_T = 76.86, $E_T(30)$ = 40.07); 1,2-dibromoethane (P_T = 75.04, $E_T(30)$ = 38.3) versus 1,2-dichloroethane (P_T = 76.45, $E_T(30)$ = 41.3). It is likely because a bromo atom is more polarizable and less electronegative than a chloro atom.

dx.doi.org/10.1021/jo400586w | *J. Org. Chem.* 2013, 78, 5925−5931

Table 1. Electronic Absorption and Emission Maxima of *o*-1 Measured in 51 Solvents at Room Temperature and the Corresponding P_T, $E_T(30)$, Z, and $\delta\Delta G^{\ddagger}$ Values of the Solvents

solvent	λ_{abs} (nm)	λ_{em}[a] (nm)	P_T (kcal/mol)	$E_T(30)$ (kcal/mol)	Z[b](kcal/mol)	$\delta\Delta G^{\ddagger}$[c] (kcal/mol)
Alkanes, Alkenes, Cycloalkanes, and Cycloalkenes						
n-pentane	383.5		74.55	31.0		
n-hexane	383.0		74.65	31.0		
cyclohexane	383.0	436(1)	74.65	30.9	60.1	
cyclohexene	376.0		76.04	32.2		
Haloalkanes						
dichloromethane	372.0		76.86	40.7	64.2	2.59
dibromomethane	376.0		76.04	39.4	62.8	
trichloromethane	377.0		76.84	39.1	63.2	
bromotrichloromethane	385.0		74.26	34.8		
1,2-dichloroethane	374.0		76.45	41.3	63.4	1.35
1,2-dibromoethane	381.0		75.04	38.3	60.0	
Alkylarenes						
benzene	381.0		75.04	34.3	54.0	4.92
toluene	383.7		74.51	33.9		
m-xylene	385.9		74.09	n/a		
p-xylene	382.0		74.85	33.1		
Heteroarenes						
pyridine	372.0		76.86	40.5	64.0	
2-chloropyridine	375.1		76.22	41.9		
Aliphatic Monoalcohols						
methanol	354.2		80.72	55.4	83.6	−3.34
ethanol (95% v/v)	353.9		80.79	52.6		
2,2,2-trichloroethanol	352.0		81.22	54.1		
1-propanol	360.9		79.22	50.7	78.3	−1.66
3-phenyl-1-propanol	367.0		77.90	48.5		
allyl alcohol	356.0		80.31	51.9		
1-butanol	367.0		77.90	49.7	77.7	−1.4
(+/−)-2-butanol	367.0		77.90	47.1		
1-pentanol	367.0		77.90	49.1		
Aliphatic Polyalcohol						
(+/−)-1,2-propanediol	355.0		80.54	54.1		
Aliphatic and Cycloaliphatic Ethers						
diethyl ether	376.1		76.02	34.5	5.72	
diisopropyl ether	376.6		75.92	34.1		
diethylene glycol dimethyl ether	372.9		76.67	38.6		
tetrahydrofuran	374.0	434(1)	76.45	37.4	58.8	3.34
1,4-dioxane	372.0		76.86	36.0	64.55	3.08
Aliphatic Ketones						
acetone	368.0		77.69	42.2	65.7	1.84
2-butanone	369.0		77.48	41.3		
4-methyl-2-pentanone	372.0		76.86	39.4		
Carboxylic Acids and Anhydrides						
acetic acid	353.0		80.99	51.7	79.2	−2.52
acetic anhydride	367.0		77.90	43.9		
Aliphatic and Aromatic Esters						
ethyl acetate	372.2		76.82	38.1	64.0	4.02
n-butyl acetate	374.0		76.45	38.5		
methyl acrylate	371.7		76.92	38.8		
N-methyl(pyrrolidin-2-one) (NMP)	370.0		77.27	42.2	0.57	
formamide	358.0		79.86	55.8	83.3	−5.66
N,*N*-dimethylformamide (DMF)	367.0		77.90	43.2	68.5	0.0
Aliphatic Nitriles						
acetonitrile	367.0	432(1)	77.90	45.6	71.3	0.18
trichloroacetonitrile	376.0		76.04	40.0		
Aliphatic and Aromatic Amines						
diethylamine	373.0		76.65	35.4		
triethylamine	386.0		74.07	32.1		
N,*N*-dimethylaniline	376.0		76.04	36.5		

dx.doi.org/10.1021/jo400586w | J. Org. Chem. 2013, 78, 5925−5931

Table 1. continued

solvent	λ_{abs} (nm)	λ_{em}[a] (nm)	P_T (kcal/mol)	$E_T(30)$ (kcal/mol)	Z[b](kcal/mol)	$\delta\Delta G^{\ddagger}$[c] (kcal/mol)
			Phosphorus Compounds			
phosphoric acid	355.0		80.54			
			Sulfur Compounds			
dimethyl sulfoxide (DMSO)	367.00	432(3)	77.90	45.1	70.2	0.62
			Water and Heavy Water			
water	348	425(0.7)	82.16	63.1	91.8	−9.56
deuterium oxide	348		82.16	62.8		

[a]Emission wavelength with the fluorescence quantum yield ($\phi_f \times 10^{-3}$) inside the parentheses. [b]References 4c and 17. [c]Reference 18.

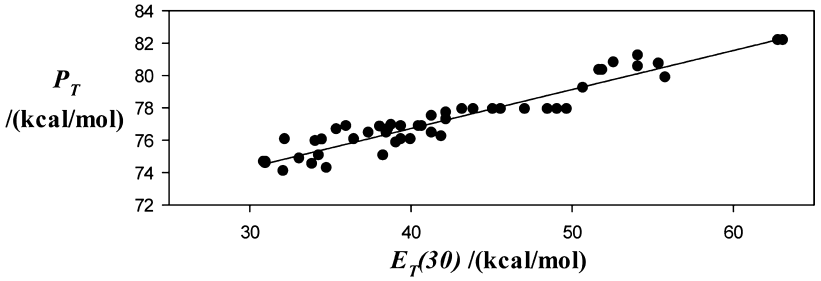

Figure 4. Linear correlation between the P_T and $E_T(30)$ values, measured in 48 solvents of different polarity at 25 °C with the correlation equation of $P_T = (0.2411)[E_T(30)] + 67.083$.

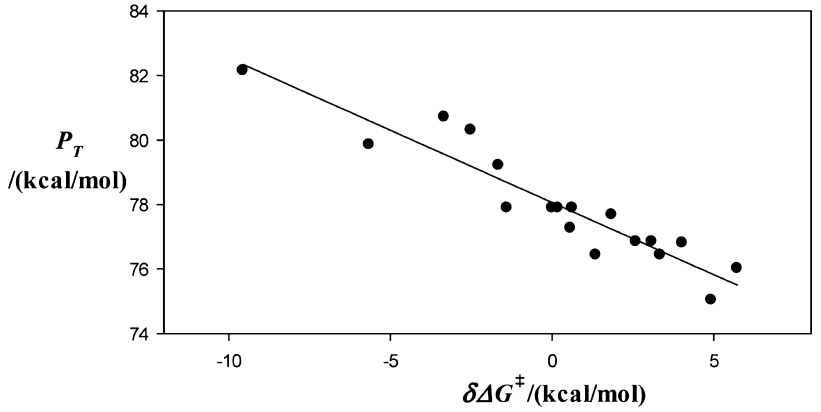

Figure 5. Linear correlation between the P_T scale and the Gibbs energies of activation of the solvolysis of 2-chloro-2-methylpropane in the 18 solvents of different polarity, taken from ref 18; $\delta\Delta G^{\ddagger} = \Delta G^{\ddagger}$ (DMF as reference solvent); the correlation equation: $P_T = (-0.4477)(\delta\Delta G^{\ddagger}) + 78.065$.

The π^* scale has a problem to accurately measure the polarity of hydrogen-bonding-donor (HBD) solvents.[19] On the contrary, the P_T scale registers the specific hydrogen-bonding solute/solvent interactions in HBD solvents as well as the $E_T(30)$ scale[1c] does. For example, the polarity of alkyl alcohol decreases as the alkyl chain length increases, such as methanol ($P_T = 80.72$, $E_T(30) = 55.4$), 1-propanol ($P_T = 79.22$, $E_T(30) = 50.7$), 1-butanol ($P_T = 77.90$, $E_T(30) = 49.7$), and 1-pentanol ($P_T = 77.90$, $E_T(30) = 49.1$). A HBD solvent is usually more polar than the corresponding non-HBD solvent, such as 1-pentanol ($P_T = 78.12$, $E_T(30) = 49.1$) versus diethyl ether ($P_T = 76.02$, $E_T(30) = 34.5$); diethylamine ($P_T = 76.65$, $E_T(30) = 35.4$) versus triethylamine ($P_T = 74.07$, $E_T(30) = 32.1$); formamide ($P_T = 79.86$, $E_T(30) = 55.8$) versus *N*,*N*-dimethylformamide (DMF) ($P_T = 77.90$, $E_T(30) = 43.2$).

It is practically impossible to find a solvent scale that is universally useful for all kinds of solute−solvent interactions.[1c] However, many empirical parameters of solvent polarity derived from similar probe molecules are linearly correlated with each other.[1c] Hence, one may use the correlation between two empirical solvent polarity scales as a tool to know if the two empirical parameters of solvent polarity register similar probe/solvent interactions. For example, the π^* scale[19] is poorly correlated with the $E_T(30)$ scale[1c] with a correlation coefficient r^2 of 0.71. This is because the π^* scale is useful for nonspecific dipole/dipole and dipole/induced dipole solute−solvent interactions only, but it cannot be used for hydrogen-bonding solute−solvent interactions.[19] For the $E_T(30)$ scale, it is also useful for nonspecific dipole/dipole and dipole/induced dipole solute/solvent interactions. In addition to that, the probe of the $E_T(30)$ scale can sense hydrogen-bonding-donor (HBD) and electron-pair-acceptor (EPA) solvents but it senses electron-pair-donor (EPD) to a much lesser extent.[1c] The P_T scale is also poorly correlated with the π^* scale with a correlation coefficient r^2 of 0.54, but it is well correlated with the $E_T(30)$ scale with a correlation coefficient r^2 of 0.90 (Figure 4). It implies that the P_T scale registers nonspecific dipole/dipole and dipole/induced dipole as well as specific hydrogen-bonding and EPA/EPD

dx.doi.org/10.1021/jo400586w | J. Org. Chem. 2013, 78, 5925−5931

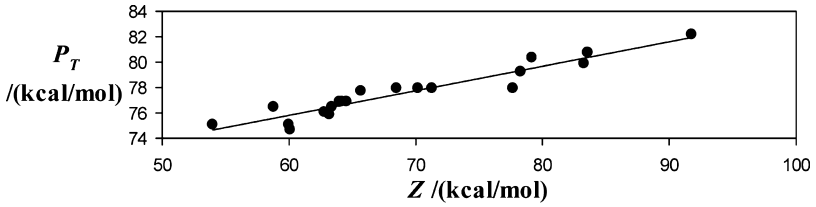

Figure 6. Linear correlation between the P_T and the Z scale,[4c,17] measured in 21 solvents of different polarity at 25 °C, with the correlation equation of $P_T = (0.193)(Z) + 64.233$.

solute/solvent interactions much closer to the $E_T(30)$ scale than the π^* scale.

The P_T scale is correlated well with the Gibbs free energy of activation[18] of the solvolysis of 2-chloro-2-methylpropane, which is a kinetically derived empirical solvent polarity parameter and has been used to introduce the Y scale of solvent ionizing power (Figure 5). This implies that the P_T scale registers the solute/solvent interactions that are similar to those of the Y scale,[18] which can sense solvent dipolarity and solvent hydrogen-bond donor acidity.

The P_T scale is also correlated well with the Z scale,[4c,17] which was based on the intermolecular charge-transfer absorption of 1-ethyl-4-(methoxycarbonyl)pyridinium iodide in various solvents (Figure 6). This implies that the P_T scale registers the solute/solvent interactions that are similar to those of the Z scale,[4c,17] which also sense dipolarity and hydrogen-bond acidity of solvents.

The question is: is it really necessary to introduce a new solvent polarity scale in addition to the many already existing scales, with the respect to the fact that the new P_T scale correlates well with the Z and $E_T(30)$ scale? There is one new aspect which possibly leads to a positive answer to this question: the new probe dye contains an intramolecular hydrogen bond, which can be broken in hydrogen-bond-accepting (HBA) solvents, giving a new intermolecular solute/solvent hydrogen bond, with corresponding changes in the electronic absorption spectrum. Therefore, the P_T scale includes also to a certain extent the HBA-properties of a solvent, which is not measured by the Z and $E_T(30)$ values. Actually, the major structural difference between the probe molecule of the P_T scale and the probe molecules of the $E_T(30)$, Y, and Z scale is that the probe molecule of the P_T scale is a hydrogen-bond donor, which allows the P_T scale to sense HBA solvents. The P_T scale cannot get a better fit with the $E_T(30)$, Y, or Z scale probably because of this major structural difference.

The probe molecule of the $E_T(30)$ scale is a betaine dye, whose charge-transfer absorption disappears in stronger acidic solvents like acetic acid because of protonation, so it is not a good probe for acidic solvents.[1c] The $E_T(30)$ values of acidic solvents were deduced from the Z scale, which can be measured in acidic solvents and shows good linear correlation with the $E_T(30)$ scale.[1c] On the contrary, our probe molecule, *o*-**1**, of the P_T scale can be used to measure the solute/solvent interactions with acidic solvents, such as acetic acid and phosphoric acid.

The probe molecule of the P_T scale still has some room to get improved in order for the lowest energy electronic absorption band to appear at a longer wavelength and to be shifted hypsochromically with increasing solvent polarity to as large an extent as possible. We hope the probe molecule, *o*-**1**, of the P_T scale can trigger the generation of even better twisting-based spectroscopic indicators for solvent polarity in the future.

CONCLUSION

This twisting-based spectroscopic measure of solvent polarity, the P_T scale, correlates well with the $E_T(30)$, Y, and Z scale. It is caused by two combined mechanisms. The first is the solvent-dependent intramolecular charge-transfer absorption that displays a regular hypsochromic band shift in polar solvents. The second is that the solvation of the probe molecule, *o*-**1**, in polar solvents overcomes its intramolecular hydrogen bonding, causing a bond twisting in the C_2-C_7 bond, where both HOMO and HOMO-1 are antibonding but LUMO is bonding. The bond twisting stabilizes both the HOMO and HOMO-1 but destabilizes the LUMO, leading to the hypsochromic shift of the lowest energy electronic absorption band ($\pi-\pi^*$ charge-transfer transition). The P_T scale successfully provides an empirical measurement of the solvent polarity and registers nonspecific dipole/dipole and dipole/induced dipole solute/solvent interactions, as well as specific hydrogen-bond and EPA/EPD solute/solvent interactions.

EXPERIMENTAL SECTION

Materials and Methods. The *o*-**ABDI** is known and was prepared according to the literature method.[10] All solvents were ordered from fine chemical companies and were of spectrophotometric grade or had the highest purity in the market. Before the measurement of the electronic absorption spectrum of *o*-**1**, all solvents were dried with activated 4 Å molecular sieves. The concentration of *o*-**1** in all 51 solvents used for electronic absorption measurement was 3.0×10^{-5} M. High-resolution mass (HRMS) measurements were obtained with a magnetic-electric sector mass analyzer.

(Z)-4-[2-(Acetamino)benzylidene]-1,2-dimethyl-(1H, 4H)-imidazol-5-one (o-1). To *o*-**ABDI** (215 mg, 1 mmol) dissolved in 3 mL of dried THF was added acetic anhydride (204 mg, 2 mmol). The mixture was stirred in a nitrogen atmosphere at room temperature for 15 h. The solution was quenched by 10 mL of water. The quenched solution was extracted with ethyl acetate. The organic layer was separated from the aqueous layer, dried with anhydrous sodium sulfate and concentrated by a rotary evaporator. The crude product was purified by column chromatography with hexane/ethyl acetate (1:1) as a mobile phase to get *o*-**1** (219 mg, 0.85 mmol), and the yield was 85%: ^{1}H NMR ($CDCl_3$, 300 MHz) δ 2.21 (s, 3H, CH_3), 2.40 (s, 3H, CH_3), 3.22 (s, 3H, CH_3), 7.09 (t, J = 7.3 Hz, 1H, PhH), 7.15 (s, 1H, CH), 7.38–7.46 (m, 2H, PhH), 8.36 (d, J = 8.3 Hz, 1H, PhH), 12.34 (br s, 1H, NH); ^{13}C NMR ($CDCl_3$, 75 MHz) δ 15.5, 24.5, 26.9, 122.9, 123.6, 123.7, 128.3, 132.2, 135.1, 135.9, 138.0, 160.4, 169.0, 169.2; HRMS (EI, M^+) m/z calcd for $C_{14}H_{15}N_3O_2$ 257.1164, found 257.1169.

ASSOCIATED CONTENT

Supporting Information

Energy, dipole moment, redundant internal coordinates, and ^{1}H and ^{13}C NMR and HMQC spectra of *o*-**1**, as well as the ^{1}H and ^{13}C NMR spectra of *o*-**ABDI**. This material is available free of charge via the Internet at http://pubs.acs.org.

dx.doi.org/10.1021/jo400586w | J. Org. Chem. 2013, 78, 5925–5931

AUTHOR INFORMATION

Corresponding Author

*E-mail: kssung@mail.ncku.edu.tw.

Notes

The authors declare no competing financial interest.

ACKNOWLEDGMENTS

We thank the National Science Council of Taiwan for financial support (NSC101-2113-M-006-001-MY3).

REFERENCES

(1) (a) Reichardt, C. *Pure Appl. Chem.* **2008**, *80*, 1415−1432. (b) Reichardt, C. *Pure Appl. Chem.* **2004**, *76*, 1903−1919. (c) Reichardt, C. *Chem. Rev.* **1994**, *94*, 2319−2358. (d) Reichardt, C.; Asharin-Fard, S.; Blum, A.; Eschner, M.; Mehranpour, A.-M.; Milart, P.; Niem, T.; Schafer, G.; Wilk, M. *Pure Appl. Chem.* **1993**, *65*, 2593−2601. (e) Reichardt, C.; Dimroth, K. *Z. Anal. Chem.* **1966**, *215*, 344−350.

(2) Meyer, K. H. *Ber. Dtsch. Chem. Ges.* **1914**, *47*, 826−832.

(3) (a) Bentley, T. W.; Llewellyn, G. *Prog. Phys. Org. Chem.* **1990**, *17*, 121−158. (b) Grunwald, E.; Winstein, S. *J. Am. Chem. Soc.* **1948**, *70*, 846−854.

(4) (a) Larsen, J. W.; Edwards, A. G.; Dobi, P. *J. Am. Chem. Soc.* **1980**, *102*, 6780−6783. (b) Kosower, E. M. *An Introduction to Physical Organic Chemistry*; Wiley: New York, 1968. (c) Kosower, E. M. *J. Am. Chem. Soc.* **1958**, *80*, 3253−3260. (d) Kosower, E. M. *J. Am. Chem. Soc.* **1958**, *80*, 3261−3266. (e) Kosower, E. M. *J. Am. Chem. Soc.* **1958**, *80*, 3267−3270. (f) Kosower, E. M.; Skorcz, J. A.; Schwarz, W. M.; Patton, J. W. *J. Am. Chem. Soc.* **1960**, *82*, 2188−2191.

(5) (a) Brooker, L. G. S.; Craig, A. C.; Heseltine, D. W.; Jenkins, P. W.; Lincoln, L. L. *J. Am. Chem. Soc.* **1966**, *87*, 2443−2450. (b) Kamlet, M. J.; Abboud, J.-L. M.; Taft, R. W. *J. Am. Chem. Soc.* **1977**, *99*, 6027−6038. (c) Kamlet, M. J.; Abboud, J.-L. M.; Taft, R. W. *J. Am. Chem. Soc.* **1977**, *99*, 8325−8327. (d) Buncel, E.; Rajagopal, S. *J. Org. Chem.* **1989**, *54*, 798−809. (e) Manuta, D. M.; Lees, A. J. *Inorg. Chem.* **1983**, *22*, 3825−3828. (f) Manuta, D. M.; Lees, A. J. *Inorg. Chem.* **1986**, *25*, 3212−3218.

(6) (a) Kucherak, O. A.; Richert, L.; Mely, Y.; Klymchenko, A. S. *Phys. Chem. Chem. Phys.* **2012**, *14*, 2292−2300. (b) Dsouza, R. N.; Pischel, U.; Nau, W. M. *Chem. Rev.* **2011**, *111*, 7941−7980. (c) Saito, R.; Matsumura, Y.; Suzuki, S.; Okazaki, N. *Tetrahedron* **2010**, *66*, 8273−8279. (d) Lopez, M.; Velasco, D.; Lopez-Calahorra, F.; Julia, L. *Tetrahedron Lett.* **2008**, *49*, 5196−5199. (e) Xing, Y.; Lin, H.; Wang, F.; Lu, P. *Sens. Actuators B* **2006**, *114*, 28−31. (f) Kosower, E. M. *Acc. Chem. Res.* **1982**, *15*, 259−266. (g) Scherer, T.; Hielkema, W.; Krijnen, B.; Hermant, R. M.; Eijckelhoff, C.; Kerkhof, F.; Ng, A. K. F.; Verleg, R.; van der Tol, E. B.; Brouwer, A. M.; Verhoeven, J. W. *Recl. Trav. Chim. Pays-Bas* **1993**, *112*, 535−548.

(7) Turro, N. J.; Ramamurthy, V.; Scaiano, J. C. *Modern Molecular Photochemistry of Organic Molecules*; University Science Publishers: New York, 2010.

(8) (a) Kudo, K.; Momotake, A.; Kanna, Y.; Nishimura, Y.; Arai, T. *Chem. Commun.* **2011**, *47*, 3867−3869. (b) Kudo, K.; Momotake, A.; Tanaka, J. K.; Miwa, Y.; Arai, T. *Photochem. Photobiol. Sci.* **2012**, *11*, 674−678.

(9) Frisch, M. J.; Trucks, G. W.; Schlegel, H. B.; Scuseria, G. E.; Robb, M. A.; Cheeseman, J. R.; Montgomery, J. A., Jr.; Vreven, T.; Kudin, K. N.; Burant, J. C.; Millam, J. M.; Iyengar, S. S.; Tomasi, J.; Barone, V.; Mennucci, B.; Cossi, M.; Scalmani, G.; Rega, N.; Petersson, G. A.; Nakatsuji, H.; Hada, M.; Ehara, M.; Toyota, K.; Fukuda, R.; Hasegawa, J.; Ishida, M.; Nakajima, T.; Honda, Y.; Kitao, O.; Nakai, H.; Klene, M.; Li, X.; Knox, J. E.; Hratchian, H. P.; Cross, J. B.; Adamo, C.; Jaramillo, J.; Gomperts, R.; Stratmann, R. E.; Yazyev, O.; Austin, A. J.; Cammi, R.; Pomelli, C.; Ochterski, J. W.; Ayala, P. Y.; Morokuma, K.; Voth, G. A.; Salvador, P.; Dannenberg, J. J.; Zakrzewski, V. G.; Dapprich, S.; Daniels, A. D.; Strain, M. C.; Farkas, O.; Malick, D. K.; Rabuck, A. D.; Raghavachari, K.; Foresman, J. B.; Ortiz, J. V.; Cui, Q.; Baboul, A. G.; Clifford, S.; Cioslowski, J.; Stefanov, B. B.; Liu, G.; Liashenko, A.; Piskorz, P.; Komaromi, I.; Martin, R. L.; Fox, D. J.; Keith, T.; Al-Laham, M. A.; Peng, C. Y.; Nanayakkara, A.; Challacombe, M.; Gill, P. M. W.; Johnson, B.; Chen, W.; Wong, M. W.; Gonzalez, C.; Pople, J. A. *Gaussian 03, Revision A.1*; Gaussian, Inc.: Pittsburgh, PA, 2003.

(10) Chen, Y.-H.; Lo, W.-J.; Sung, K. *J. Org. Chem.* **2013**, *78*, 301−310.

(11) (a) Zhu, X.-M.; Zhang, S.-Q.; Zheng, X.; Phillips, D. L. *J. Phys. Chem. A* **2005**, *109*, 3086−3093. (b) Vaswani, H. M.; Hsu, C.-P.; Head-Gordon, M.; Fleming, G. R. *J. Phys. Chem. B* **2003**, *107*, 7940−7946.

(12) The dipole moment for the optimized structure of the electronic ground-state of *o*-**1** at the B3PW91/6-311++G(3df,2p)// B3LYP/6-31+G* level is 5.1248 D. The dipole moment for the optimized structure of the first singlet excited state of *o*-**1** at the B3LYP/def-SV(P) level is 3.1338 D, which was calculated with the Turbomole version 6.0.

(13) Chen, Y.-H. Ph.D. Thesis; National Cheng Kung University: Tainan, Taiwan, 2012.

(14) Klessinger, M.; Michl, J. *Excited States and Photochemistry of Organic Molecules*; VCH Publishers: New York, 1995.

(15) (a) Soriano-Correa, C.; del Valle, F. J. O.; Munoz-Losa, A.; Galvan, I. F.; Martin, M. E.; Aguilar, M. A. *J. Phys. Chem. B* **2010**, *114*, 8961−8970. (b) Chang, J.; Lenhoff, A. M.; Sandler, S. I. *J. Phys. Chem. B* **2007**, *111*, 2098−2106. (c) Wong, S. E.; Bernacki, K.; Jacobson, M. *J. Phys. Chem. B* **2005**, *109*, 5249−5258.

(16) Galamba, N. *J. Phys. Chem. B* **2012**, *116*, 5242−5250.

(17) (a) Griffiths, T. R.; Pugh, D. C. *Coord. Chem. Rev.* **1979**, *29*, 129−211. (b) Medda, K.; Chatterjee, P.; Chandra, A. K.; Bagchi, S. *J. Chem. Soc., Perkin Trans. 2* **1992**, 343−346. (c) Medda, K.; Chatterjee, P.; Pal, M.; Bagchi, S. *J. Solution Chem.* **1990**, *19*, 271−287.

(18) Abraham, M. H.; Grellier, P. L.; Nasehzadeh, A.; Walker, R. A. C. *J. Chem. Soc., Perkin Trans. 2* **1988**, 1717−1719.

(19) Laurence, C.; Nicolet, P.; Dalati, M. T.; Abboud, J.-L.; Notario, R. *J. Phys. Chem.* **1994**, *98*, 5807−5816.